

Tree-Ring Evidence of Increasing Drought Risks over the Past Five Centuries amidst Projected Flood Intensification in the Kabul River Basin (Afghanistan and Pakistan)

Khan Nasrullah¹, Nguyen Hung T.T², Galelli Stefano³, and Cherubini Paolo⁴

¹Laboratory of Plant Ecology Department of Botany, University of Malakand

²Columbia University

³Singapore University of Technology and Design

⁴WSL Swiss Federal Research Institute

November 16, 2022

Abstract

Increased flood risks have been projected in the Kabul River Basin, but with large uncertainties. To place future changes in a long-term perspective, we produce a 501-year precipitation reconstruction for the basin using seven tree-ring chronologies of *Cedrus deodara*, *Picea smithiana*, and *Pinus gerardiana* from the Hindukush Mountains, a monsoon-shadow area. The reconstruction proves robust over rigorous cross-validations ($R^2 = 0.62$, RE = 0.61, CE = 0.53). The full reconstruction (1517–2018) shows heterogeneous changes in the precipitation distribution: there is a weak increasing trend in the median annual precipitation, no apparent trend in the 50-year maximum precipitation, and, importantly, a steadily decreasing trend in 50-year minimum precipitation. In other words, our reconstruction shows that drought risks have been increasing over the past five centuries. Drought risks, compounded with projected flood intensification, pose significant threats for the transboundary river. Future water management decisions should factor in past long-term climate variability.

Tree-Ring Evidence of Increasing Drought Risks over the Past Five Centuries amidst Projected Flood Intensification in the Kabul River Basin (Afghanistan and Pakistan)

Nasrullah Khan¹, Hung T. T. Nguyen², Stefano Galelli^{2,3}, and Paolo Cherubini^{2,4,5}

¹Department of Botany, University of Malakand, Chakdara Dir Lower (P.O. Box 18800), Khyber Pakhtunkhwa Pakistan

²Tree Ring Laboratory, Lamont-Doherty Earth Observatory, Columbia University, Palisades, New York, USA

³Pillar of Engineering Systems and Design, Singapore University of Technology and Design, Singapore

⁴WSL Swiss Federal Institute for Forest, Snow and Landscape Research, Birmensdorf Switzerland

⁵Faculty of Forestry, University of British Columbia, Vancouver BC, Canada

Key Points:

- Robust, skillful precipitation reconstruction of the Kabul River Basin from tree rings
- Heterogeneous trends in the bulk and the extremes of precipitation distribution
- Drought risks have been increasing over the past five centuries amidst projected flood intensification

Corresponding author: Hung T. T. Nguyen, hnguyen@ldeo.columbia.edu

Abstract

Increased flood risks have been projected in the Kabul River Basin, but with large uncertainties. To place future changes in a long-term perspective, we produce a 501-year precipitation reconstruction for the basin using seven tree-ring chronologies of *Cedrus deodara*, *Picea smithiana*, and *Pinus gerardiana* from the Hindukush Mountains, a monsoon-shadow area. The reconstruction proves robust over rigorous cross-validations ($R^2 = 0.62$, $RE = 0.61$, $CE = 0.53$). The full reconstruction (1517–2018) shows heterogeneous changes in the precipitation distribution: there is a weak increasing trend in the median annual precipitation, no apparent trend in the 50-year maximum precipitation, and, importantly, a steadily decreasing trend in 50-year minimum precipitation. In other words, our reconstruction shows that drought risks have been increasing over the past five centuries. Drought risks, compounded with projected flood intensification, pose significant threats for the transboundary river. Future water management decisions should factor in past long-term climate variability.

Plain Language Summary

The Kabul River is a transboundary river spanning northern Afghanistan and Pakistan. It is an important tributary of the Indus, one of the world’s largest rivers with intensive water withdrawals for human use. With climate change, the Kabul River is projected to have more frequent and larger floods, but the projections are very uncertain. To have a better understanding of these future projections, we need to look at how the region’s climate has changed in the past. Tree rings are a valuable source of information to serve that need. Using tree ring data from the Hindukush Mountains, western Himalaya, we reconstruct five century of precipitation (rainfall) history for the Kabul River Basin. From the reconstruction, we observe that while a “typical” year is indeed getting wetter (as indicated by the median precipitation), dry years are getting drier, as shown by the progression of the years with the lowest precipitation. Thus, the risks of severe droughts are increasing. Our results imply that the Kabul River Basin is facing both floods and drought risks, and these are significant threats to the water security of the basin.

1 Introduction

The Indus River system is one of the largest basins in the world (Best, 2019). Yet, owing to the extensive man-made water storage and withdrawal infrastructure along its course, the river is nearly depleted (Sharma et al., 2010). Shared by four countries—Pakistan, Afghanistan, China, and India—the basin supports a population of about 300 million people (Laghari et al., 2012). Among these, the semi-arid countries of Afghanistan and Pakistan are particularly reliant on the Indus, and are facing acute water and food shortages as well as threats of transboundary water conflicts (Akhtar & Iqbal, 2017; Atef et al., 2019). Located in the Indus headwaters, and originated from the Hindu Kush–Karakoram Mountains, the Kabul River is an important tributary of the Indus, accounting for about 10% of the annual flow, and supplying water directly to the Afghan capital, Kabul (Lashkaripour & Hussaini, 2008). The Kabul River has experienced intensive human-induced environmental changes in the last 40-years (Ahmadullah & Dongshik, 2015), and new dams are planned to be built (Yousaf, 2017). Development in both the Afghan and Pakistani sides of the river, such as dam construction and increase in built-up and cultivated areas, may worsen transboundary water conflicts (Akhtar & Iqbal, 2017; Atef et al., 2019; Taraky et al., 2021).

On top of the increasing water stresses due to human activities, the Kabul River Basin faces an uncertain future because of climate change. Climate models predict consistent warming and drying trends in the Indus Basin, but with considerable uncertainties surrounding the magnitude and spatial pattern of these changes (Shakir et al., 2010; Z. Ahmad et al., 2012; Wi et al., 2015). Despite the overall projected drying trend in the Indus Basin, little change has been observed in annual precipitation in the Indus headwaters over the past decades (Khattak et al., 2011), and most climate models project an increase in precipitation in the Kabul River particularly (Iqbal et al., 2018). The combination of higher precipitation and enhanced snowmelt due to warming is thus projected to increase flood frequency and intensity in the Kabul River Basin (Iqbal et al., 2018; S. Ahmad et al., 2021).

A major factor that confounds projections of water resources availability in the region is a peculiar phenomenon named the “Karakoram Anomaly”, where glaciers in the Karakoram Mountains gain masses and experience higher frequencies of glacial surges, contradicting the overall trends in High-Mountain Asia and other glaciated regions worldwide (Hewitt, 2005). The cause of this anomaly remains undetermined, although several plausible causes have been put forth (see e.g., Yao et al., 2012; Kapnick et al., 2014; Forsythe et al., 2017; Farinotti et al., 2020). Furthermore, while evidence from tree rings suggests that the anomaly may have been stable for centuries (Zafar et al., 2016), the future stability of the phenomenon is highly uncertain with global warming (Farinotti et al., 2020). As the Indus derives a significant amount of runoff from the Karakoram Mountains, these uncertainties greatly hamper the assessment of future surface water availability in the region.

Against this back drop of increasing water stress and uncertain hydroclimatic projections, we turn our attention to the past hydroclimatic variability of the Kabul River Basin. This knowledge could help constraint future projections and put recent and future changes in a long-term perspective. Here, we present a five-century annual precipitation reconstruction for the Kabul River Basin using seven old-growth conifer chronologies developed from both the Afghan and Pakistani sides of the basin. Our reconstruction provides a long-term record of moisture input to the basin—an important step towards understanding the long-term changes in the water cycle and their implications to regional water management.

2 Materials and Methods

2.1 Study Area and Sampled Species

We sampled three coniferous species on the Hindu Kush Mountains (Figure 1): *Cedrus deodara* (Roxb.) G. Don (commonly known as Himalayan cedar), *Picea smithiana* (Wall. Boiss; Himalayan spruce) and *Pinus gerardiana* (Wall. Ex. Lamb.; Chilgoza pine). Additional details of the sites are provided in Table S1. *Pinus gerardiana* is typically found in the inner semi-arid regions of the north-western Himalaya, between 1,800 and 3,000 m asl (Singh et al., 2021), with low summer monsoon rainfall but high winter snowpack. *Cedrus deodara* is found through the western Himalayas at elevations between 1,500 and 3,300 m asl. This species forms mixed stands with *Picea smithiana* at 2,500 m and above, whereas at lower elevations usually forms associations with *Abies pindrow* and *Pinus wallichiana* (Champion et al., 1965). *Cedrus deodara* generally prefers sites with low humidity and high winter snowpack (Raizada & Sahni, 1960; Sahni, 1990). In addition, well-drained soils, good amount of winter snowfall, and not too abundant summer rain are its fundamental ecological requirements (Brandis, 1906; Champion & Seth, 1968). In the study area, the three species were found growing on steep rocky slopes in Chitral Gol National Park, Bumburat Kalash valley, and Lowari Top (Figure 1) with very thin soil cover. All the three species grow in open stands; this might be due to very long-term (e.g., millennial time scales) anthropogenic interventions, as the local people depends on these forests (Khan et al., 2013). As a result, tree-ring patterns of the sampled trees should not be influenced much by stand dynamics such as suppression and release due to inter-tree competition.

2.2 Tree Ring Data

During the sampling phase, care was taken to select healthy trees without visible injuries or fire scars. Cores were sampled at breast height (1.3 m), dried, glued, and sanded following standard dendrochronological protocols. Samples were cross-dated with the skeleton plot method (Stokes & Smiley, 1996; Speer, 2010) and measured with a LINTAB tree-ring measurement station (Rinntech, Heidelberg Germany). Measurements were then statistically validated using the software COFECHA (Holmes, 1983).

Finally, we detrended and standardized the chronologies using the program ARSTAN (Cook, 1985). We found that the Friedman variable span smoother was generally most suitable for removing non-climatic signals from our series. In a few cases where the Friedman variable span smoother showed a lack of fit, the cubic smoothing spline (Cook and Peters 1981) was used. From the output of ARSTAN, three chronologies can be derived—i.e., standard, residual, and ARSTAN—but for climate reconstruction we selected the residual chronology, which is the average of residuals from autoregressive modeling of the detrended measurements. The final chronologies and their subsample signal strength (SSS; Wigley et al., 1984) are shown in Figure S1, and other statistics are reported in Table S2. Following recommendations by Buras (2017), we used SSS rather than the expressed population signal (EPS) to determine the length of chronology to retain. The SSS was computed using the R package `dp1R` (Bunn, 2008). Wigley et al. (1984) recommended a threshold of 0.85 (and this is the value commonly used in the literature); however, they noted that it was only a guideline. Here, in order to maximize the usable length of tree ring data, we chose a threshold of 0.6, at which point the chronologies still appear stable.

2.3 Climate Data

We obtained monthly precipitation and temperature data for the Chitral meteorological station (Figure 1b). Our record covers the period 1965–2018, among the longest records in Pakistan. The station is located in a monsoon shadow area, away from sum-

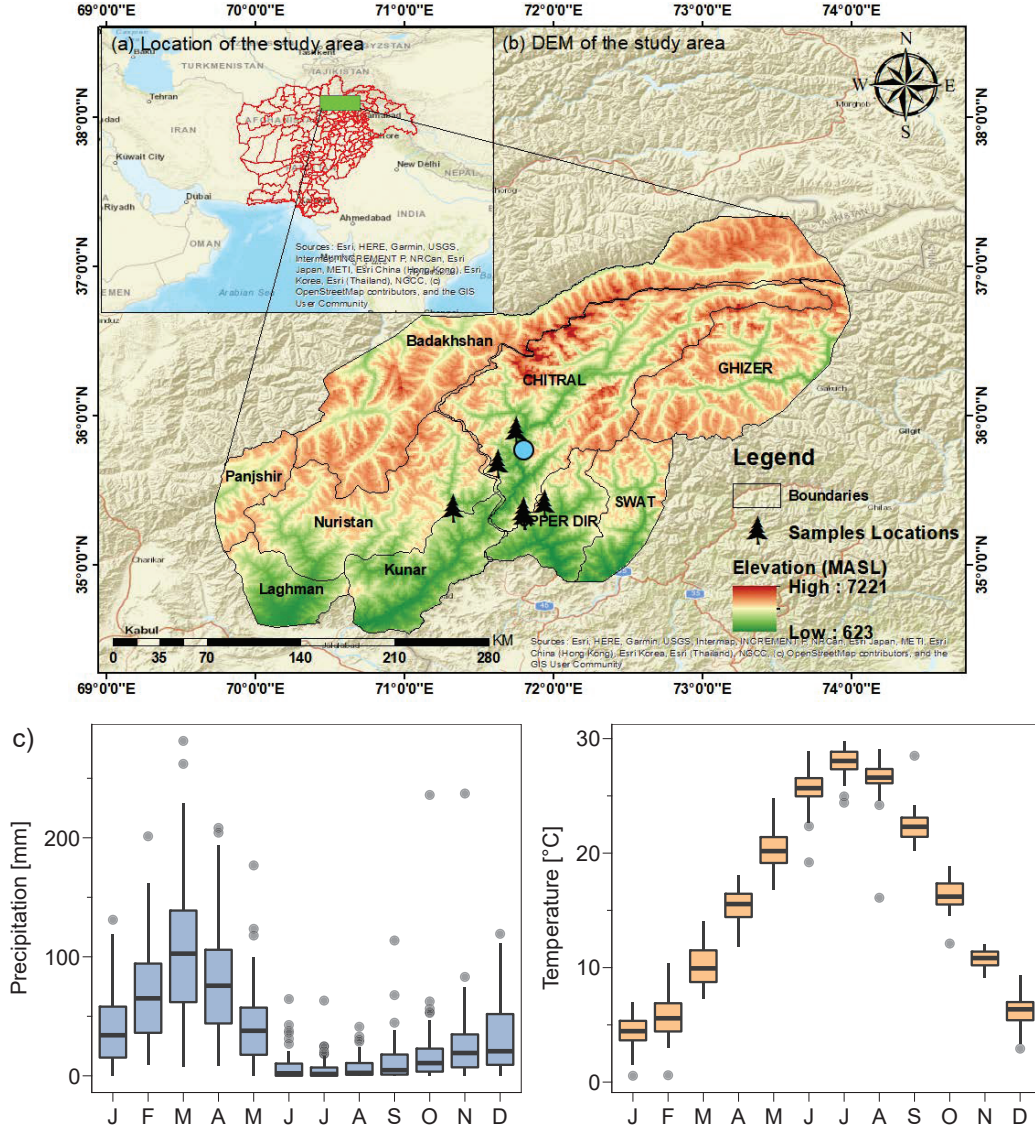


Figure 1. a) Location of the study region. b) Map of the study area showing the sampling sites, Chitral meteorological station (blue dot), as well as the topography. c) Monthly distribution of precipitation and temperature at Chitral.

mer monsoon winds. Precipitation is predominantly delivered by western disturbances originating from the Mediterranean Sea (Ridley et al., 2013; Iqbal et al., 2018). Precipitation peaks in March, and the wet season spans from December to May, contributing more than 70% of the total annual precipitation (Figure 1c). June to August are usually the driest months. As temperatures are mostly above freezing, precipitations are typically in liquid form.

2.4 Climate–Growth Relationship

To determine the target reconstruction season, we calculated the correlations between each chronology and the precipitation of each month from prior year’s January to current year’s December (Figure 2). All sites display a generally consistent correla-



–6–

converge to those of the observed data. This gap filling strategy has been implemented with good results in earlier reconstruction works (e.g., Stagge et al., 2018; Nguyen et al., 2021). The results of the gap filling procedure are shown in Figure S2.

After gap filling, we conducted the final PCA. Only PC1 has an eigenvalue greater than one, but PC2 and PC3's eigenvalues are very close to one (0.96 and 0.93, respectively; Figure S3). Therefore, PC2 and PC3 were also considered candidate predictors. We then carried out backward stepwise linear regression, which resulted in PC1 and PC2 being retained in the final model.

The reconstruction was cross-validated with a moving-block cross-validation procedure, in which contiguous, rolling blocks of k years were left out for verification while the model was calibrated with the remaining data (Nguyen et al., 2020; Higgins et al., 2022). Here k was set as 14 years, or 25% of the data length. The commonly used metrics Reduction of Error (RE) and Coefficient of Efficiency (CE) (Cook & Kairiukstis, 1990; Nash & Sutcliffe, 1970) were used to assess the reconstruction quality.

Finally, the reconstructed time series was bias-corrected using the quantile mapping method from the R package `qmap` (Gudmundsson, 2016; Robeson et al., 2020). This step is important to ensure that the instrumental period's portion of the reconstruction has a similar distribution to that of the instrumental data. If the distributions were not matched, subsequent statistical comparisons between the paleo and instrumental periods would not be fair.

2.6 Trend and Drought Analyses

To understand how precipitation in the Kabul River Basin has changed over a long term, we analyzed the trends in median precipitation and extremes in a rolling window manner. For each 50-year window, we obtained the maximum, median, and minimum precipitation from the bias-corrected time series, then calculated the trends in these rolling values, and tested these trends with the Mann-Kendall test. To account for serial autocorrelations, we employed the trend-free pre-whitening procedure (Yue & Wang, 2002) before performing the Mann-Kendall test, and estimated the slope of the trend with Sen's method (Sen, 1968). These steps were conducted using the R package `modifiedmk` (Patakamuri & O'Brien, 2021).

For the purpose of drought analysis, we define a meteorological drought event as one that starts with two consecutive years of negative precipitation anomalies, and ends with two consecutive years of positive anomalies (Herweijer et al., 2007; Coats et al., 2013). The last two years with positive anomalies are not counted towards the duration. Anomalies are calculated with respect to the mean precipitation over the full reconstruction (1517–2018). A drought's severity is taken as the worst precipitation anomaly during its duration.

3 Results

3.1 Model Performance

The mean performance scores of the reconstruction across 30 cross-validation runs are: $R^2 = 0.62$, RE = 0.61 and CE = 0.53. In all cross-validation runs, RE and CE are always positive (Figure S4). The reconstruction explains 62% of variance in precipitation, and the model shows robustly good skills under a rigorous cross-validation scheme. This is also reflected by the reconstruction trajectory, which matches observation closely (Figure 3a). However, agreement between the reconstruction and observations are not as good in the extremes, particularly in the wettest years. This leads to a mismatch between the density of the reconstruction and that of the instrumental data (Figure 3b): frequencies of extremely dry and extremely wet years are underestimated by the recon-

struction. This is a common limitation of tree-ring-based reconstructions (see e.g. Robeson et al., 2020). There are two possible causes: first, the climate–growth relationship may become nonlinear at the extremes (Torbensohn & Stagge, 2021); second, trees may not be able to capture moisture inputs beyond the soil saturation level (Nguyen et al., 2021). These shortcomings can be mitigated by bias correction. We found that the bias-corrected precipitation distribution matches very closely with observations, much better than the uncorrected distribution does (Figure 3b).

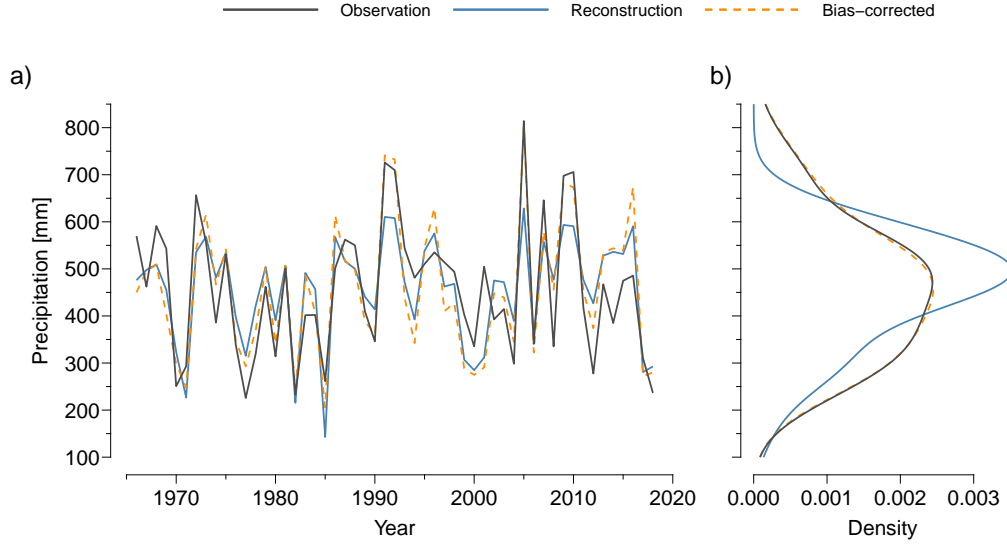


Figure 3. a) Comparison between observed, reconstructed, and bias-corrected water-year precipitation time series for the instrumental period (1965–2018). b) Comparison between the densities of observed, reconstructed, and bias-corrected water year precipitation. All densities are calculated for the instrumental period only.

3.2 Five Centuries of Precipitation Variability

We found no significant trend in 50-year maximum precipitation ($p = 0.64$), and a statistically significant but very small increasing trend in median annual precipitation (0.04 mm/year, $p \approx 0$). There is, however, a significant and considerable decreasing trend in 50-year minimum precipitation (−0.17 mm/year, $p \approx 0$) (Figure 4a). This decreasing trend caused a clear shift in the precipitation in the second half of the record compared to the first half (Figure 4b): the left tail of the distribution decreased from about 270 mm in the first half to only about 200 mm in the second half (a 26% reduction). Median precipitation increased from 425 mm to 438 mm. The right tail of the distribution remains almost the same. However, that does not mean maximum precipitation did not change. Between 1650–1700, and between 1925–2018, there were multiple years with extremely high precipitation, while maximum precipitation was lower from 1700–1900.

The negative trend of minimum precipitation prompted us to examine droughts in the reconstruction. Based on precipitation anomalies (Figure 4c), and using drought definitions outlined in Section 2.6, we determined the duration and severity of each drought event in the past five centuries (Figure 4d). The three most severe droughts in the record all happened during the latter half (1718–2018), one of which (1805–1822) was the longest

on record. While drought duration remains the same, drought severity has increased because of the decline in minimum precipitation.

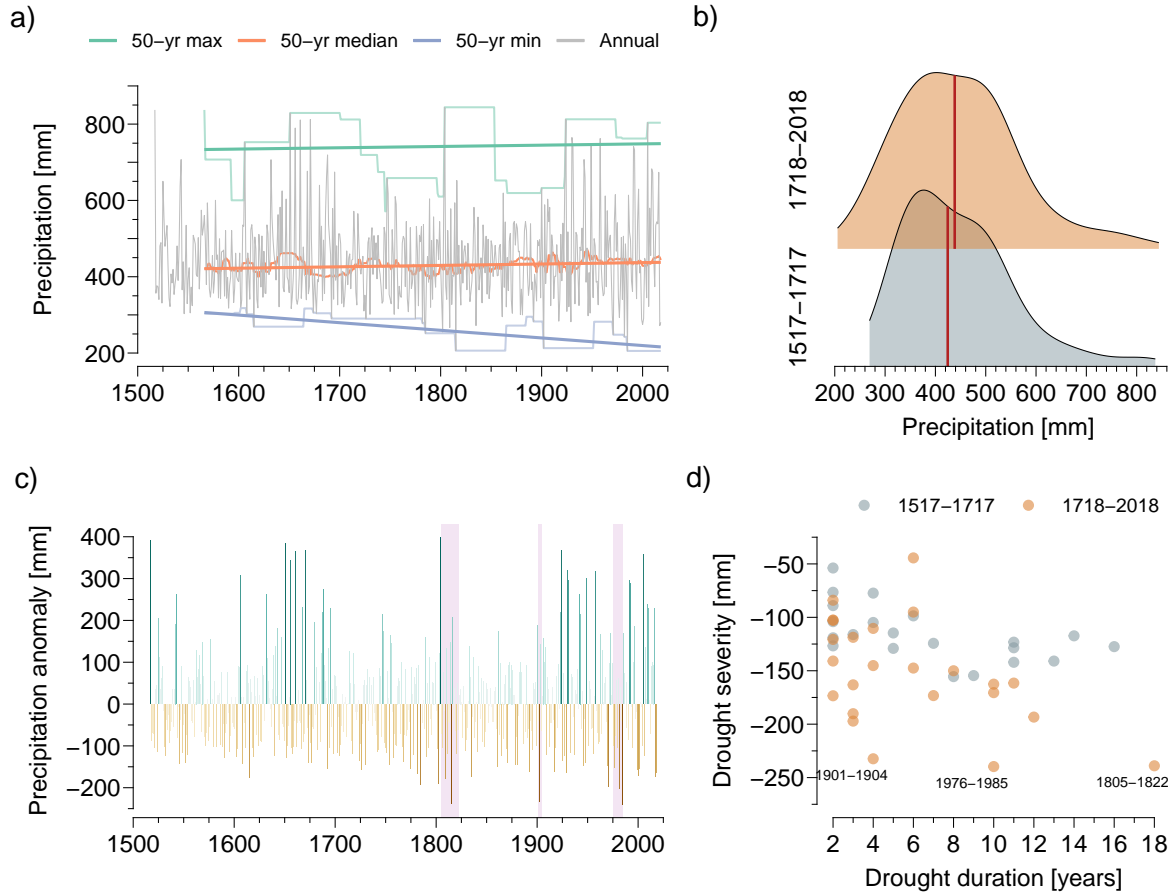


Figure 4. a) Time series of the full reconstruction, as well as its maximum, median, and minimum in rolling 50-year windows. The trends in maximum, median, and minimum are also shown with thick straight lines. b) Precipitation distributions in the first and second halves of the reconstruction. The red vertical lines denote the mean in each period. c) Time series of precipitation anomalies. Highlighted are the three most severe droughts (1805–1822, 1901–1904, and 1976–1985). d) Scatterplot of drought duration and severity. The three most severe droughts are annotated.

4 Discussion and Conclusions

Using seven tree-ring width chronologies from the Hindu Kush Mountains, we reconstructed five centuries of precipitation history for the Kabul River Basin (Pakistan and Afghanistan). The reconstruction is skillful and robust under rigorous cross-validation. Trend analyses of the reconstruction revealed heterogeneous changes: no trend in maximum precipitation, statistically significant but small increasing trend in median precipitation, and lastly, significant and considerable decline in annual precipitation. These heterogeneous trends show that when analyzing hydrological changes, it is important to look at the full distribution shifts, rather than just one portion of the distribution, be it the bulk or the extremes.

Our reconstruction reveals that meteorological drought risks have been increasing over the past five centuries: droughts in the last 250 years are more severe than those in the preceding 250 years. This result is disconcerting, amidst projections of increased precipitation and floods for the basin as reported in the literature (S. Ahmad et al., 2021). The main moisture source for the basin is western disturbances in the Mediterranean Sea, which have been projected to occur more frequently in the Karakoram (Ridley et al., 2013). Modeling studies involving hydrological models forced with outputs from global circulation models have projected flood intensification for the Kabul River as a whole (Iqbal et al., 2018), but with declining streamflow for some sub-catchments (Shakir et al., 2010; Naeem et al., 2013). There are still large uncertainties to be resolved in future projections, as discrepancies among climate models have been shown to be greater than calibration uncertainties in hydrological models (Wi et al., 2015).

Even when future uncertainties are resolved and flood intensification turns out to be true, our findings do not contradict such projections, because floods and droughts are not mutually exclusive—floods act on short time scales (hours or days) while droughts manifest on longer time scales (months, years, or longer). On the contrary, our results corroborate that the water cycle is intensifying (Huntington, 2006; Seager et al., 2010; Yu et al., 2020), as evidenced by the increased variability in precipitation particularly since 1800s in our reconstruction. “Typical” years, as indicated by median precipitation, are getting wetter but dry years, indicated by minimum precipitation, are getting drier. Our findings are of concerns for the transboundary management of the Kabul River Basin. Facing both flood and drought risks, water management decisions across the basin need to consider climate variability at multiple time scales, and tree-ring-based reconstructions is a valuable source of information to serve that need.

5 Open Research

All data and code necessary to reproduce this paper are available on GitHub at <https://github.com/ntthung/chitral-precip> (DOI: 10.5281/zenodo.6941584). An HTML notebook, rendered from R Markdown, that documents the full process of analysis, including code, discussion, and outputs, is included in the Supporting Information (Code S1). Additionally, tree ring data will be made available on the International Tree Ring Data Bank.

Acknowledgments

Nasrullah Khan’s visit to Paolo Cherubini’s laboratories was funded by the Swiss National Science Foundation (Project IZSEZ0_186442). Hung Nguyen is supported by the Lamont-Doherty Postdoctoral Fellowship.

References

- Ahmad, S., Jia, H., Chen, Z., Li, Q., Yin, D., Israr, M., ... Ashraf, A. (2021, September). Effects of climate and land use changes on stream flow of Chitral river basin of northern highland Hindu-Kush region of Pakistan. *Journal of Hydro-environment Research*, 38, 53–62. doi: 10.1016/j.jher.2021.08.001
- Ahmad, Z., Hafeez, M., & Ahmad, I. (2012, September). Hydrology of mountainous areas in the upper Indus Basin, Northern Pakistan with the perspective of climate change. *Environmental Monitoring and Assessment*, 184(9), 5255–5274. doi: 10.1007/s10661-011-2337-7
- Ahmadullah, R., & Dongshik, K. (2015). Assessment of Potential Dam Sites in the Kabul River Basin Using GIS. *International Journal of Advanced Computer Science and Applications (ijacsa)*, 6(2). doi: 10.14569/IJACSA.2015.060213
- Akhtar, S. M., & Iqbal, J. (2017, March). Assessment of emerging hydrological,

- water quality issues and policy discussion on water sharing of transboundary Kabul River. *Water Policy*, 19(4), 650–672. doi: 10.2166/wp.2017.119
- Atef, S. S., Sadeqinazhad, F., Farjaad, F., & Amatya, D. M. (2019, March). Water conflict management and cooperation between Afghanistan and Pakistan. *Journal of Hydrology*, 570, 875–892. doi: 10.1016/j.jhydrol.2018.12.075
- Best, J. (2019). Anthropogenic stresses on the world’s big rivers. *Nature Geoscience*, 12(1), 7–21. doi: 10.1038/s41561-018-0262-x
- Brandis, D. (1906). *Indian trees: An account of trees, shrubs, woody climbers, bamboos and palms indigenous or commonly cultivated in the British Indian empire*. Dehradun: Constable.
- Bunn, A. G. (2008). A dendrochronology program library in R (dplR). *Dendrochronologia*, 26(2), 115–124. doi: 10.1016/j.dendro.2008.01.002
- Buras, A. (2017, June). A comment on the expressed population signal. *Dendrochronologia*, 44, 130–132. doi: 10.1016/j.dendro.2017.03.005
- Champion, H. G., & Seth, S. K. (1968). *A revised survey of the forest types of India*. New Delhi: Manager of publications.
- Champion, H. G., Seth, S. K., & Khattak, G. M. (1965). *Forest Types of Pakistan*. Peshawar, Pakistan: Pakistan Forest Institute.
- Coats, S., Smerdon, J. E., Seager, R., Cook, B. I., & González-Rouco, J. F. (2013, October). Megadroughts in Southwestern North America in ECHO-G Millennial Simulations and Their Comparison to Proxy Drought Reconstructions. *Journal of Climate*, 26(19), 7635–7649. doi: 10.1175/JCLI-D-12-00603.1
- Cook, E. R. (1985). *A time series analysis approach to tree ring standardisation* (Unpublished doctoral dissertation). The University of Arizona.
- Cook, E. R., & Kairiukstis, L. A. (Eds.). (1990). *Methods of Dendrochronology*. Dordrecht: Springer Netherlands. doi: 10.1007/978-94-015-7879-0
- Farinotti, D., Immerzeel, W. W., de Kok, R. J., Quincey, D. J., & Dehecq, A. (2020, January). Manifestations and mechanisms of the Karakoram glacier Anomaly. *Nature Geoscience*, 13(1), 8–16. doi: 10.1038/s41561-019-0513-5
- Forsythe, N., Fowler, H. J., Li, X.-F., Blenkinsop, S., & Pritchard, D. (2017, September). Karakoram temperature and glacial melt driven by regional atmospheric circulation variability. *Nature Climate Change*, 7(9), 664–670. doi: 10.1038/nclimate3361
- Gudmundsson, L. (2016). *Qmap: Statistical transformations for post-processing climate model output. R package version 1.0-4*.
- Herweijer, C., Seager, R., Cook, E. R., & Emile-Geay, J. (2007, April). North American Droughts of the Last Millennium from a Gridded Network of Tree-Ring Data. *Journal of Climate*, 20(7), 1353–1376. doi: 10.1175/JCLI4042.1
- Hewitt, K. (2005, November). The Karakoram Anomaly? Glacier Expansion and the ‘Elevation Effect,’ Karakoram Himalaya. *Mountain Research and Development*, 25(4), 332–340. doi: 10.1659/0276-4741(2005)025[0332:TKAGEA]2.0.CO;2
- Holmes, R. L. (1983). Computer assisted quality control. *Tree-Ring Bulletin*, 43, 69–78.
- Huntington, T. G. (2006, March). Evidence for intensification of the global water cycle: Review and synthesis. *Journal of Hydrology*, 319(1), 83–95. doi: 10.1016/j.jhydrol.2005.07.003
- Iqbal, M. S., Dahri, Z. H., Querner, E. P., Khan, A., & Hofstra, N. (2018, April). Impact of Climate Change on Flood Frequency and Intensity in the Kabul River Basin. *Geosciences*, 8(4), 114. doi: 10.3390/geosciences8040114
- Josse, J., & Husson, F. (2016). missMDA: A Package for Handling Missing Values in Multivariate Data Analysis. *Journal of Statistical Software*, 70(1). doi: 10.18637/jss.v070.i01
- Kapnick, S. B., Delworth, T. L., Ashfaq, M., Malyshev, S., & Milly, P. C. D. (2014, November). Snowfall less sensitive to warming in Karakoram than in Himalayas due to a unique seasonal cycle. *Nature Geoscience*, 7(11), 834–840.

- doi: 10.1038/ngeo2269
- Khan, N., Ahmed, M., & Shaukat, S. (2013, September). Climatic signal in tree-ring chronologies of *Cedrus deodara* from Chitral Hindukush Range of Pakistan. *Geochronometria*, 40(3), 195–207. doi: 10.2478/s13386-013-0115-8
- Khattak, M. S., Babel, M. S., & Sharif, M. (2011, February). Hydro-meteorological trends in the upper Indus River basin in Pakistan. *Climate Research*, 46(2), 103–119. doi: 10.3354/cr00957
- Laghari, A. N., Vanham, D., & Rauch, W. (2012, April). The Indus basin in the framework of current and future water resources management. *Hydrology and Earth System Sciences*, 16(4), 1063–1083. doi: 10.5194/hess-16-1063-2012
- Lashkaripour, G. R., & Hussaini, S. A. (2008, September). Water resource management in Kabul river basin, eastern Afghanistan. *The Environmentalist*, 28(3), 253–260. doi: 10.1007/s10669-007-9136-2
- Naeem, U. A., Hashmi, H. N., Habib-ur-Rehman, & Shakir, A. S. (2013, January). Flow trends in river Chitral due to different scenarios of glaciated extent. *KSCE Journal of Civil Engineering*, 17(1), 244–251. doi: 10.1007/s12205-013-1978-1
- Nash, J. E., & Sutcliffe, J. V. (1970, April). River flow forecasting through conceptual models part I — A discussion of principles. *Journal of Hydrology*, 10(3), 282–290. doi: 10.1016/0022-1694(70)90255-6
- Nguyen, H. T. T., Galelli, S., Xu, C., & Buckley, B. M. (2021). Multi-Proxy, Multi-Season Streamflow Reconstruction with Mass Balance Adjustment. *Water Resources Research*, 57(8), e2020WR029394. doi: 10.1029/2020WR029394
- Patakamuri, S. K., & O'Brien, N. (2021). *Modifiedmk: Modified versions of Mann Kendall and Spearman's rho trend tests*.
- Politis, D. N., & Romano, J. P. (1994). The Stationary Bootstrap. *Journal of the American Statistical Association*, 89(428), 1303–1313. doi: 10.1080/01621459.1994.10476870
- Raizada, M., & Sahni, K. (1960). Living Indian gymnosperms. Part 1 (Cycades, Ginkgoales and Coniferales). *Indian Forest Records (Botany)*, 5(2), 73–150.
- Ridley, J., Wiltshire, A., & Mathison, C. (2013, December). More frequent occurrence of westerly disturbances in Karakoram up to 2100. *Science of The Total Environment*, 468–469, S31–S35. doi: 10.1016/j.scitotenv.2013.03.074
- Robeson, S. M., Maxwell, J. T., & Ficklin, D. L. (2020). Bias Correction of Paleoclimatic Reconstructions: A New Look at 1,200+ Years of Upper Colorado River Flow. *Geophysical Research Letters*, 47(1), 1–12. doi: 10.1029/2019GL086689
- Sahni, K. C. (1990). *Gymnosperms of India and adjacent countries*. Dehradun: Bishen Singh Mahendral Pal Singh.
- Seager, R., Naik, N., & Vecchi, G. A. (2010, September). Thermodynamic and Dynamic Mechanisms for Large-Scale Changes in the Hydrological Cycle in Response to Global Warming. *Journal of Climate*, 23(17), 4651–4668. doi: 10.1175/2010JCLI3655.1
- Sen, P. K. (1968, December). Estimates of the Regression Coefficient Based on Kendall's Tau. *Journal of the American Statistical Association*, 63(324), 1379–1389. doi: 10.1080/01621459.1968.10480934
- Shakir, A. S., Rehman, H.-u., & Ehsan, S. (2010). Climate Change Impact on River Flows in Chitral Watershed. *Pakistan Journal of Engineering and Applied Sciences*.
- Sharma, B., Amarasinghe, U., Xueliang, C., de Condappa, D., Shah, T., Mukherji, A., ... Smakhtin, V. (2010, November). The Indus and the Ganges: River basins under extreme pressure. *Water International*, 35(5), 493–521. doi: 10.1080/02508060.2010.512996
- Singh, G., Kumar, D., & Dash, A. K. (2021, May). *Pinus gerardiana* Wallichex. D. Don. -A review. *Phytomedicine Plus*, 1(2), 100024. doi: 10.1016/j.phyplu.2021.100024

- 413 Speer, J. H. (2010). *Fundamentals of tree-ring research*. University of Arizona
414 Press.
- 415 Stagge, J. H., Rosenberg, D. E., DeRose, R. J., & Rittenour, T. M. (2018). Monthly
416 paleostreamflow reconstruction from annual tree-ring chronologies. *Journal of*
417 *Hydrology*, 557, 791–804. doi: 10.1016/j.jhydrol.2017.12.057
- 418 Stokes, M. A., & Smiley, T. L. (1996). *An Introduction to Tree-Ring Dating*. Tucson,
419 Arizona: The University of Arizona Press.
- 420 Taraky, Y. M., McBean, E., Liu, Y., Daggupati, P., Shrestha, N. K., Jiang, A., &
421 Gharabaghi, B. (2021, January). The Role of Large Dams in a Transboundary
422 Drought Management Co-Operation Framework—Case Study of the Kabul
423 River Basin. *Water*, 13(19), 2628. doi: 10.3390/w13192628
- 424 Torbenson, M. C. A., & Stagge, J. H. (2021). Informing Seasonal Proxy-Based Flow
425 Reconstructions Using Baseflow Separation: An Example From the Potomac
426 River, United States. *Water Resources Research*, 57(2), e2020WR027706. doi:
427 10.1029/2020WR027706
- 428 Wi, S., Yang, Y. C. E., Steinschneider, S., Khalil, A., & Brown, C. M. (2015, Febru-
429 ary). Calibration approaches for distributed hydrologic models in poorly gaged
430 basins: Implication for streamflow projections under climate change. *Hydrology*
431 *and Earth System Sciences*, 119(2), 857–876. doi: 10.5194/hess-19-857-2015
- 432 Wigley, T. M. L., Briffa, K. R., & Jones, P. D. (1984, February). On the Average
433 Value of Correlated Time Series, with Applications in Dendroclimatology and
434 Hydrometeorology. *Journal of Applied Meteorology and Climatology*, 23(2),
435 201–213. doi: 10.1175/1520-0450(1984)023<0201:OTAVOC>2.0.CO;2
- 436 Yao, T., Thompson, L., Yang, W., Yu, W., Gao, Y., Guo, X., ... Joswiak, D. (2012,
437 September). Different glacier status with atmospheric circulations in Tibetan
438 Plateau and surroundings. *Nature Climate Change*, 2(9), 663–667. doi: 10
439 .1038/nclimate1580
- 440 Yousaf, S. (2017). Kabul River and Pak-Afghan relations. *Central Asian Journal*,
441 80, 97–112.
- 442 Yu, L., Josey, S. A., Bingham, F. M., & Lee, T. (2020). Intensification of the global
443 water cycle and evidence from ocean salinity: A synthesis review. *Annals of*
444 *the New York Academy of Sciences*, 1472(1), 76–94. doi: 10.1111/nyas.14354
- 445 Yue, S., & Wang, C. Y. (2002). Applicability of prewhitening to eliminate the influ-
446 ence of serial correlation on the Mann-Kendall test. *Water Resources Research*,
447 38(6), 4-1-4-7. doi: 10.1029/2001WR000861
- 448 Zafar, M. U., Ahmed, M., Rao, M. P., Buckley, B. M., Khan, N., Wahab, M., &
449 Palmer, J. (2016, March). Karakorum temperature out of phase with hemi-
450 spheric trends for the past five centuries. *Climate Dynamics*, 46(5-6), 1943–
451 1952. doi: 10.1007/s00382-015-2685-z

Code for *Tree-Ring Evidence of Increasing Drought Risks amidst Projected Flood Intensification in the Kabul River Basin (Afghanistan and Pakistan)* by Khan et al. (2022)

Hung Nguyen

2022-05-14

Introduction and Preparations

This document details the process of producing the results presented in **Tree-Ring Evidence of Increasing Drought Risks amidst Projected Flood Intensification in the Kabul River Basin (Afghanistan and Pakistan)** by Khan et al. (2022).

To reproduce the results, please do the following:

- This code requires R 4.1.0 and above.
- Download the code repository from the GitHub repo and extract the downloaded .zip file to your working folder.
- Open `chitral-precip.Rproj` in RStudio (**It's important to open this first so that the file path is loaded properly**).
- Install and load the following packages if you don't already have them. For package `ldsr`, please use the development version which can be installed from GitHub with

```
remotes::install_github('ntthung/ldsr')
```

```
library(dplR)      # Tree ring data processing
library(ldsr)      # Tree ring data processing
library(data.table) # Data handling
library(missMDA)    # Imputation
library(qmap)       # Bias correction
library(modifiedmk) # Trend analysis
library(ggplot2)    # Plotting
library(cowplot)    # Plotting
library(patchwork)  # Plotting
library(ggprism)    # Plotting
library(ggnewscale) # Plotting
theme_set(theme_prism(base_size = 10, base_fontface = 'plain', base_line_size = 0.2))
```

- Open `paper-code.Rmd`, which is the source code for this document.
- Follow the written details below and run the code chunks one by one.

This R Markdown is set to render both HTML and PDF outputs. To do so, please run


```
rmarkdown::render('paper-code.Rmd', output_format = 'all', output_options = list(hightlight = 'tango'))
```

For quick access to the final results please see the .csv file in **results/**.

The code utilities to support the main code are stored in the folder **R/**. We need to load them first before running the main code.

```
source('R/init.R')
source('R/correlation_functions.R')
source('R/drought_analysis_functions.R')
```

Data

Climate data

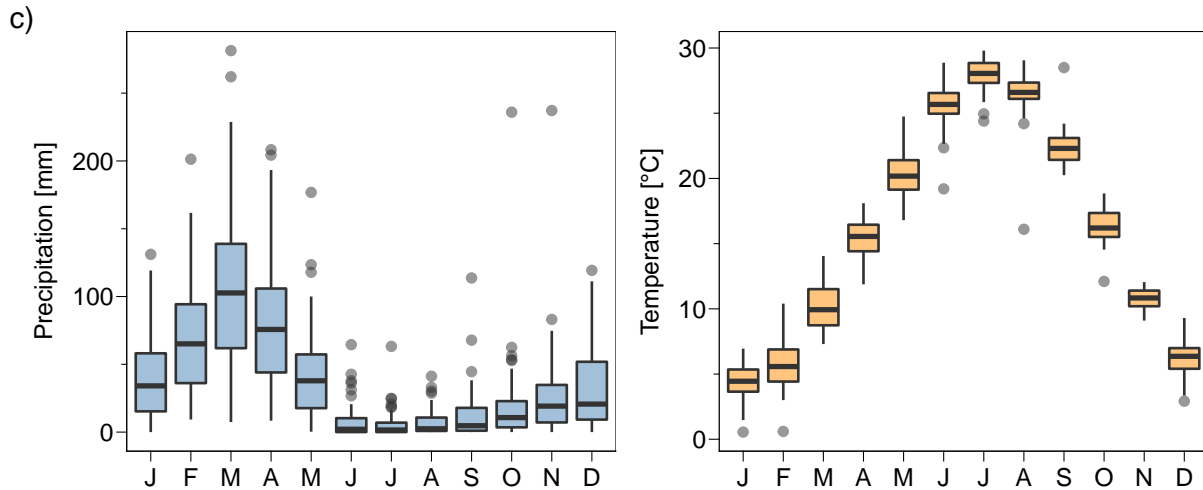
```
# Monthly temperature
TmWide <- fread('data/chitral-monthly-T.csv')
Tm <- melt(TmWide, id.var = 'year', variable.name = 'month2', variable.factor = TRUE, value.name = 'Tm')
      [, month := as.integer(month2)
      ][order(year, month)]

# Monthly precipitation
PmWide <- fread('data/chitral-monthly-P.csv')
Pm <- melt(PmWide, id.var = 'year', variable.name = 'month2', variable.factor = TRUE, value.name = 'Pm')
      [, month := as.integer(month2)
      ][order(year, month)]
```

Figure 1c

```
p1 <- ggplot(Pm) +
  geom_boxplot(aes(month2, Pm), fill = 'steelblue', alpha = 0.5) +
  labs(x = NULL, y = 'Precipitation [mm]', tag = 'c') +
  scale_x_discrete(labels = \(x) substr(x, 1, 1)) +
  scale_y_continuous(guide = guide_prism_minor()) +
  panel_border('black', 0.2)

p2 <- ggplot(Tm) +
  geom_boxplot(aes(month2, Tm), fill = 'darkorange', alpha = 0.5) +
  labs(x = NULL, y = 'Temperature [\u00b0C]') +
  scale_x_discrete(labels = \(x) substr(x, 1, 1)) +
  scale_y_continuous(guide = guide_prism_minor()) +
  panel_border('black', 0.2)
p1 + p2
```



Tree ring data

```
# Read ARSTAN outputs
crnRaw <- lapplyrbind(
  list.files('data/', '.tabs', full.names = TRUE),
  function(fn) {
    dt <- fread(fn)
    dt[, site := substr(fn, 6, nchar(fn) - 5)]
  })
setkey(crnRaw, site)
sssOut <- fread('data/sss.csv', key = 'site')
crn <- merge(crnRaw, sssOut, by = c('site', 'year'))

firstYear <- crn[sss > 0.6][, .N, by = year][N >= 4, first(year)]
lastYear <- 2018
# Use the residual chronology
crnWide <- crn[year %in% firstYear:lastYear, dcast(.SD, year ~ site, value.var = c('res'))]
```

Figure S1 - Chronology and SSS plot

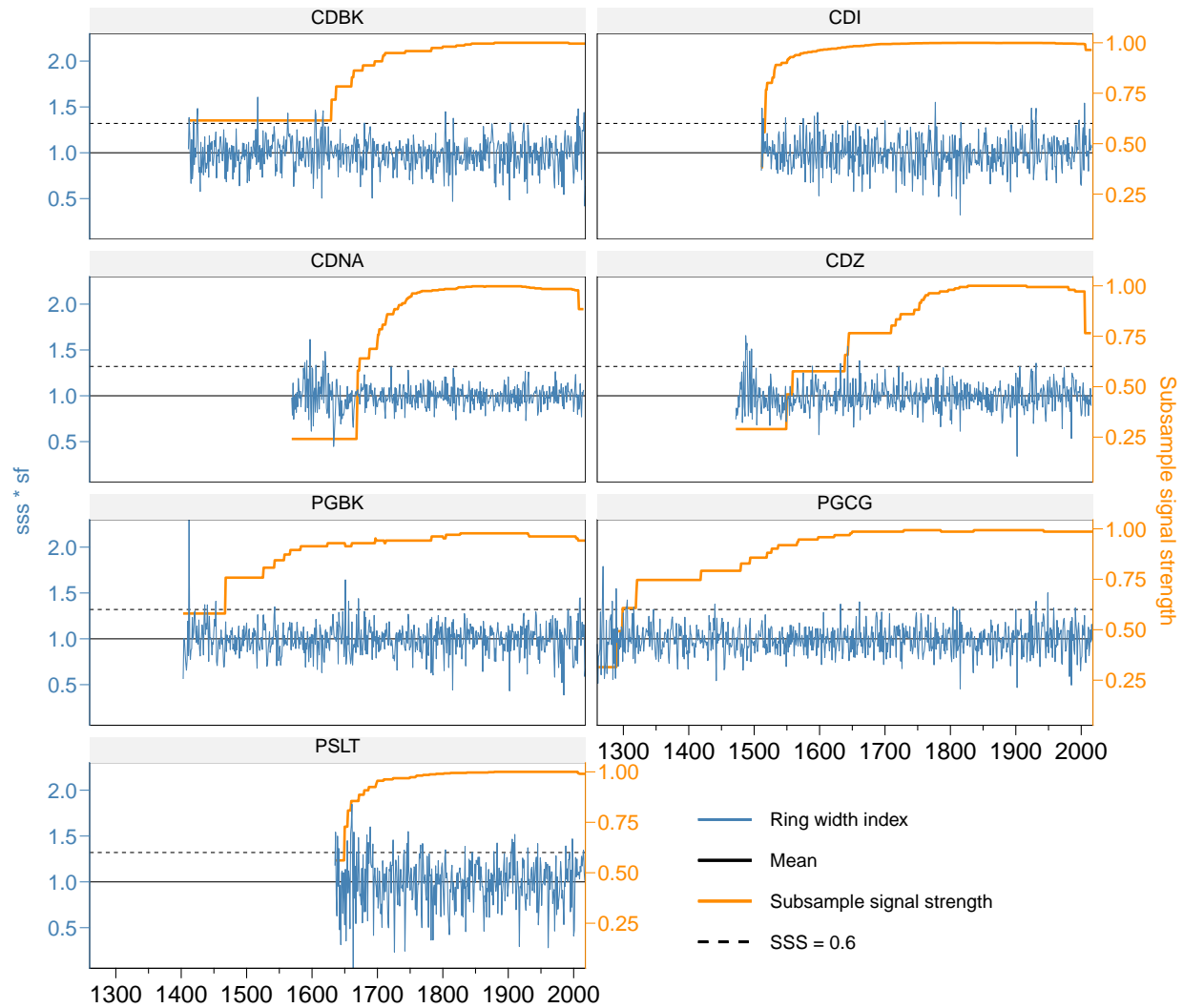
```
sf <- 2.2
ggplot(sssOut) +
  geom_hline(aes(yintercept = 1, linetype = 'Mean', color = 'Mean')) +
  # geom_hline(aes(yintercept = 0.85 * sf,
  #               # color = 'SSS = 0.85', linetype = 'SSS = 0.85')) +
  geom_hline(aes(yintercept = 0.6 * sf,
                color = 'SSS = 0.6', linetype = 'SSS = 0.6')) +
  geom_line(aes(year, sss * sf,
                col = 'Subsample signal strength',
                linetype = 'Subsample signal strength'), size = 0.5) +
  geom_line(aes(year, res,
                col = 'Ring width index',
                linetype = 'Ring width index'), crn) +
  facet_wrap(~site, ncol = 2) +
```

```

scale_x_continuous(
  name = NULL,
  breaks = seq(1300, 2000, 100),
  minor_breaks = seq(1300, 2000, 50),
  guide = guide_prism_minor(),
  expand = c(0, 0)) +
scale_y_continuous(

  sec.axis = sec_axis(~ . / sf, name = 'Subsample signal strength',
                      breaks = seq(0, 1, 0.25)),
  expand = c(0, 0)) +
scale_color_manual(
  name = NULL,
  breaks = c('Ring width index', 'Mean',
             'Subsample signal strength', 'SSS = 0.6'),
  values = c('steelblue', 'black', 'darkorange', 'black')) +
scale_linetype_manual(
  name = NULL,
  breaks = c('Ring width index', 'Mean',
             'Subsample signal strength', 'SSS = 0.6'),
  values = c(1, 1, 1, 2)) +
guides(color = guide_legend(override.aes = list(size = 0.50))) +
theme(
  strip.background = element_rect('gray95', NA),
  legend.position = c(0.75, 0.1),
  legend.key.width = unit(1, 'cm'),
  panel.border = element_rect(NA, 'black', 0.2),
  axis.ticks.y.right = element_line(color = 'darkorange'),
  axis.text.y.right = element_text(color = 'darkorange', size = 9),
  axis.title.y.right = element_text(color = 'darkorange', size = 9),
  axis.line.y.right = element_line(color = 'darkorange'),
  axis.ticks.y.left = element_line(color = 'steelblue'),
  axis.text.y.left = element_text(color = 'steelblue', size = 9),
  axis.title.y.left = element_text(color = 'steelblue', size = 9),
  axis.line.y.left = element_line(color = 'steelblue'))

```



Climate-growth relationship

First we infill the tree ring data.

```
X <- crnWide[, -'year'] |>
  as.matrix() |>
  imputePCA(ncp = 6) |>
  {\(x) x$completeObs}()
PC <- prcomp(X, scale. = TRUE)$x
Xraw <- as.matrix(crnWide[, -'year'])
impModel <- imputePCA(Xraw, ncp = 6)
Xfilled <- impModel$completeObs
Xfitted <- impModel$fittedX
colnames(Xfitted) <- colnames(Xfilled)

crnFitted <- as.data.table(as.data.frame(Xfitted))
crnFitted[, year := 1517:2018]
crnFittedLong <- melt(
```

```

  crnFitted, id.vars = 'year', variable.name = 'site', value.name = 'rwi')
crnMerge <- rbindlist(
  list(Infilled = crnFittedLong, Original = crn[, .(site, year, rwi = res)]),
  use.names = TRUE,
  idcol = 'type')

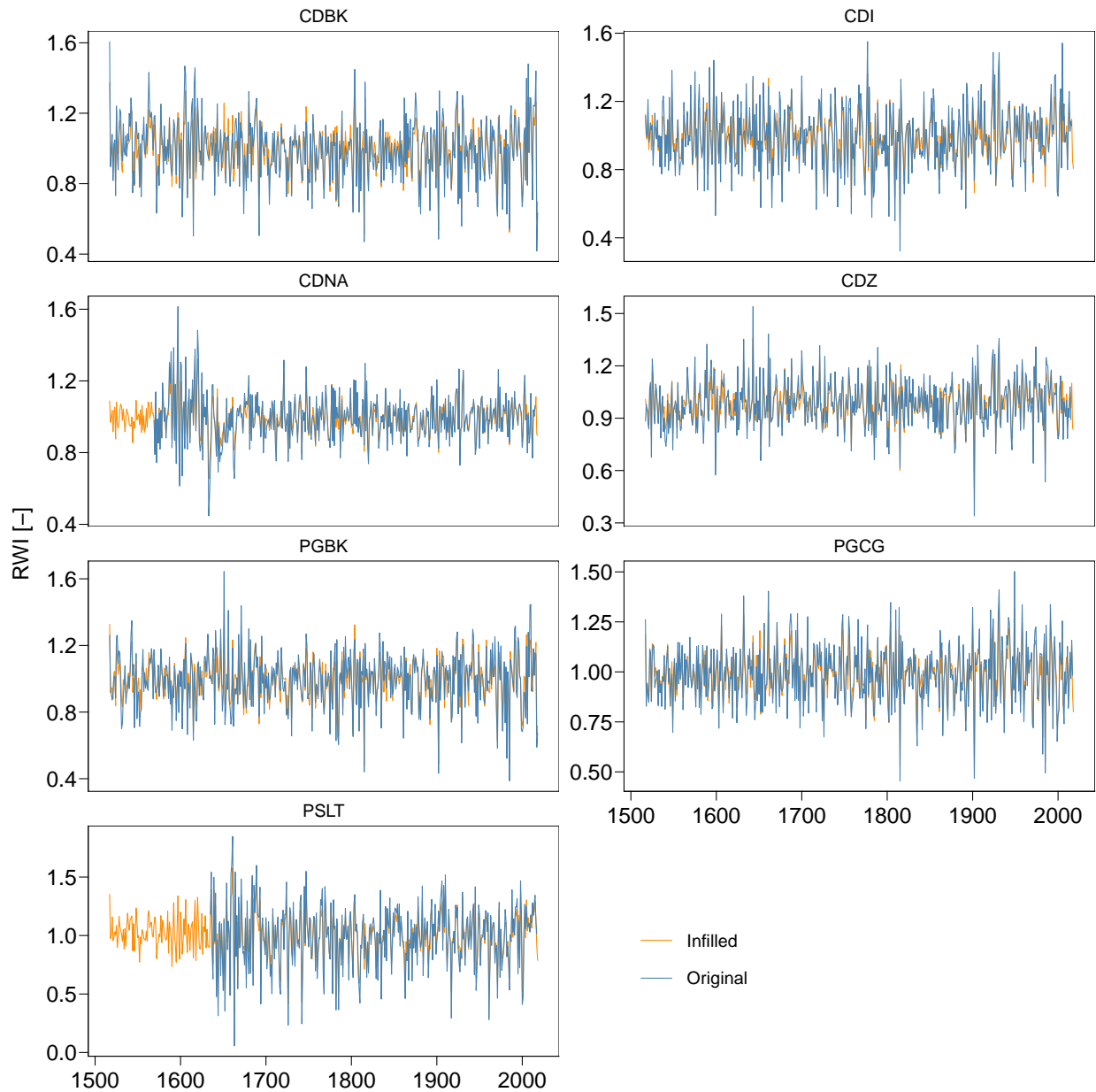
```

Figure S2

```

ggplot(crnMerge[year >= 1517]) +
  geom_line(aes(year, rwi, color = type)) +
  facet_wrap(vars(site), ncol = 2, scales = 'free_y') +
  scale_color_manual(values = c('darkorange', 'steelblue')) +
  scale_x_continuous(breaks = seq(1500, 2000, 100)) +
  labs(x = NULL, y = 'RWI [-]') +
  panel_border('black', 0.2) +
  theme(legend.position = c(0.6, 0.1))

```



Calculate bootstrapped correlations.

```
treeYears <- crnWide$year
# Current year
# Merge TR in 1965-2018 with precipitation in 1965-2018
instIndc <- which(treeYears %in% 1965:2018)
XYc <- cbind(Xfilled[instIndc, ], as.matrix(PmWide[, -'year']))

# Tree rings and previous year precipitation
# Merge TR in 1966-2018 with precipitation in 1965-2017
instIndp <- which((treeYears - 1) %in% 1965:2017) # previous year streamflow
XYp <- cbind(Xfilled[instIndp, ], as.matrix(PmWide[-.N, -'year']))

# Tree rings and next year precipitation
```

```

# Merge TR in 1963-2016 with precipitation in 1965-2018
# instIndn <- which((treeYears + 1) %in% 1965:2018) # next year streamflow
# XYn <- cbind(Xfilled[instIndn, ], as.matrix(PmWide[, -'year']))

set.seed(2022)
corDTc <- cor_boot(XYc, 1:7, 8:19, groupNames = c('site', 'month')) # current year
corDTp <- cor_boot(XYp, 1:7, 8:19, groupNames = c('site', 'month')) # current year
# corDTn <- cor_boot(XYn, 1:7, 8:19, groupNames = c('site', 'month')) # current year

corDTc[, month := paste0(month, 'c')]
corDTp[, month := paste0(month, 'p')]
# corDTn[, month := paste0(month, 'n')]

corDTPm <- rbind(corDTp, corDTc)
corDTPm[, month := factor(month, c(paste0(month.abb, 'p'), paste0(month.abb, 'c')))]

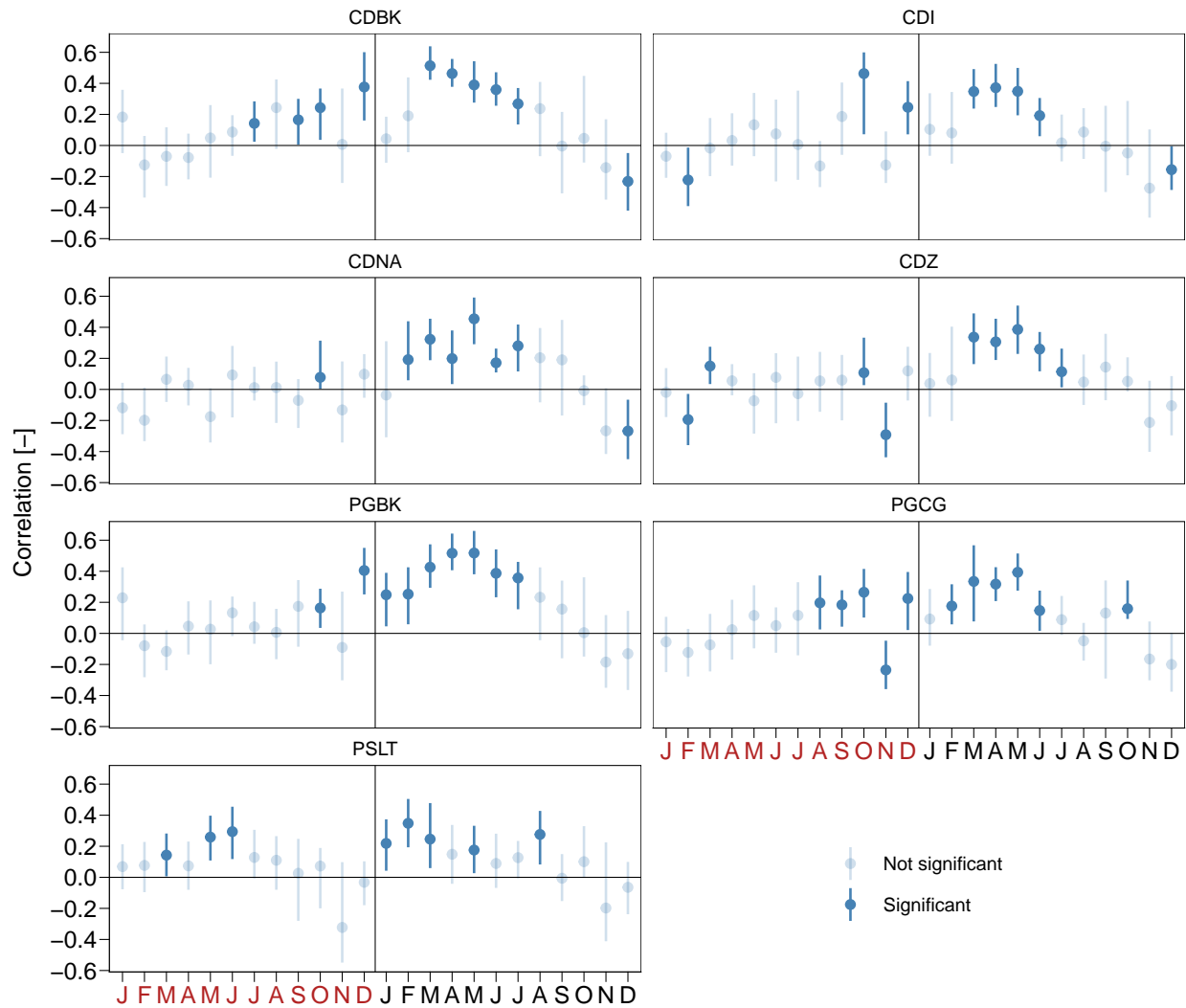
```

Figure 2

```

ggplot(corDTPm) +
  geom_linerange(
    aes(x = month, ymin = low, ymax = high, alpha = signif), color = 'steelblue') +
  geom_point(
    aes(x = month, y = rho0, alpha = signif), color = 'steelblue') +
  geom_hline(aes(yintercept = 0)) +
  geom_vline(xintercept = 12.5) +
  facet_wrap(vars(site), ncol = 2) +
  scale_x_discrete(name = NULL, labels = monthLab) +
  scale_y_continuous(name = 'Correlation [-]',
                     breaks = c(-0.6, -0.4, -0.2, 0, 0.2, 0.4, 0.6)) +
  scale_alpha_manual(
    values = c(0.25, 1), labels = c('Not significant', 'Significant')) +
  theme(
    legend.position = c(0.75, 0.1),
    axis.text.x = ggtext::element_markdown()) +
  panel_border('black', 0.2)

```

September to August precipitation reconstruction

Principal component analysis

```
PCfit <- prcomp(X, scale. = TRUE)
PC <- PCfit$x
pcDT <- as.data.table(as.data.frame(summary(PCfit)$importance),
                      keep.rownames = 'var') |>
  melt(id.vars = 'var', variable.name = 'PC')
```

Figure S3

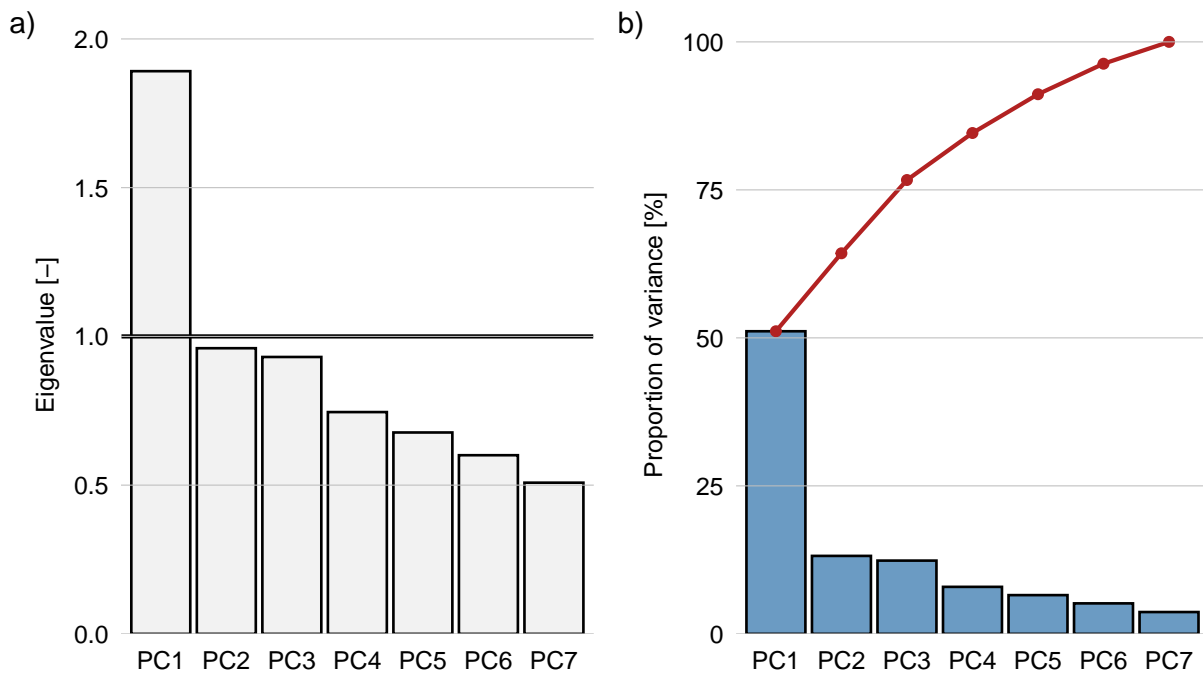
```
p1 <- ggplot(pcDT[var == 'Standard deviation']) +
  geom_col(aes(PC, value), color = 'black', fill = 'gray95') +
  geom_hline(yintercept = 1, size = 0.8) +
  scale_y_continuous(expand = expansion(add = c(0, 0.01)),
```

```

limits = c(0, 2)) +
labs(x = NULL, y = 'Eigenvalue [-]', tag = 'a') +
theme(
  panel.grid.major.y = element_line('gray'),
  panel.ontop = TRUE,
  axis.ticks = element_blank(),
  axis.line = element_blank())
p2 <- ggplot() +
  geom_col(
    aes(PC, value * 100),
    pcDT[var == 'Proportion of Variance'],
    fill = 'steelblue', color = 'black', alpha = 0.8) +
  geom_line(
    aes(PC, value * 100, group = 1),
    pcDT[var == 'Cumulative Proportion'],
    color = 'firebrick', size = 0.8) +
  geom_point(
    aes(PC, value * 100),
    pcDT[var == 'Cumulative Proportion'],
    color = 'firebrick', size = 1.6) +
  labs(x = NULL, y = 'Proportion of variance [%]', tag = 'b') +
  scale_y_continuous(expand = expansion(add = c(0, 1))) +
  theme(
    panel.grid.major.y = element_line('gray'),
    panel.ontop = TRUE,
    axis.ticks = element_blank(),
    axis.line = element_blank())

p1 + p2

```



Reconstruction

```
Pm[, year2 := fifelse(month %in% 9:12, year + 1, year)]
PSepAug <- Pm[, .(Qa = sum(Pm)), by = .(year = year2)][year %in% 1966:lastYear]
instInd <- which(firstYear:lastYear %in% PSepAug$year)

# Stepwise linear regression
DT <- cbind(PC[450:502, 1:3], Qa = PSepAug$Qa) |> as.data.frame()
step(lm(Qa ~ ., DT), direction = 'backward')
```

```
## Start: AIC=480.5
## Qa ~ PC1 + PC2 + PC3
##
##           Df Sum of Sq    RSS    AIC
## - PC3      1      496 395002 478.57
## <none>                      394506 480.50
## - PC2      1     51858 446364 485.05
## - PC1      1    302975 697481 508.70
##
## Step: AIC=478.57
## Qa ~ PC1 + PC2
##
##           Df Sum of Sq    RSS    AIC
## <none>                      395002 478.57
## - PC2      1     52713 447715 483.21
## - PC1      1    302816 697819 506.73
##
##
## Call:
## lm(formula = Qa ~ PC1 + PC2, data = DT)
##
## Coefficients:
## (Intercept)      PC1      PC2
##      459.50     -37.96      38.41
```

Build final model

```
sPC <- as.data.table(PC[, 1:2])
lmFit <- PCR_reconstruction(PSepAug, sPC, firstYear, transform = 'none')
set.seed(42)
cvFolds <- make_Z(PSepAug$Qa, frac = 0.25, contiguous = TRUE)
lmCV <- cvPCR(PSepAug, sPC, firstYear, transform = 'none',
              Z = cvFolds, use.robust.mean = FALSE)
```

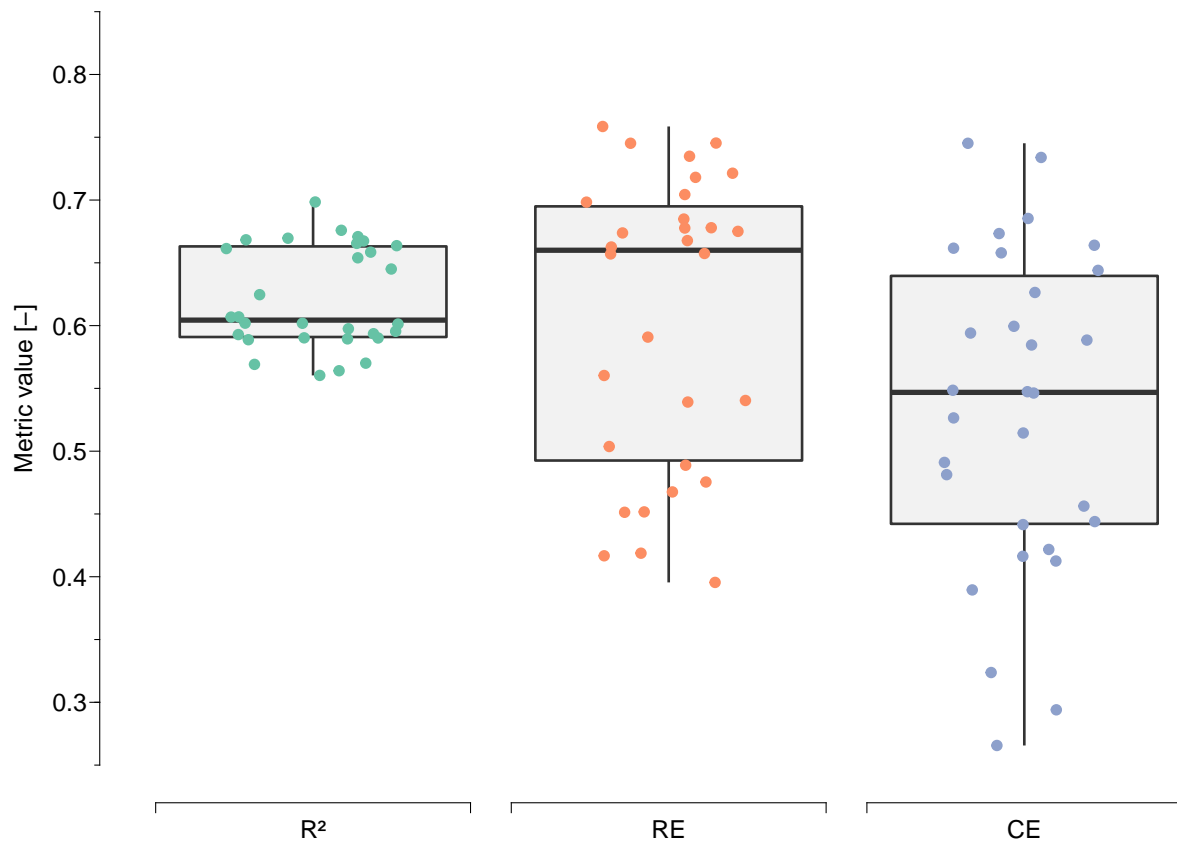
Performance scores

```
round(lmCV$metrics[, 1:3], 2)
```

```
##      R2   RE   CE
## 1: 0.62 0.61 0.53
```

Figure S4 - score distribution

```
scores <- melt(lmCV$metrics.dist[, .(R2, RE, CE)],
              measure.vars = 1:3,
              variable.name = 'metric')
ggplot(scores) +
  geom_boxplot(aes(metric, value), fill = 'grey95') +
  geom_jitter(aes(metric, value, color = metric), width = 0.25) +
  scale_color_brewer(palette = 'Set2') +
  scale_x_discrete(
    name = NULL,
    guide = guide_prism_bracket(),
    labels = c('R\u00b2', 'RE', 'CE')) +
  scale_y_continuous(
    name = 'Metric value [-]',
    limits = c(0.25, 0.85),
    breaks = seq(0.2, 0.9, 0.1),
    minor_breaks = seq(0.25, 0.85, 0.05),
    guide = guide_prism_offset_minor()) +
  theme(legend.position = 'none')
```



Final reconstruction with bias correction.

```
recFinal <- lmFit$rec
recFinal[, lp20 := dplR::pass.filt(Q, 20, 'low')]
```

```

recFinal[, lp50 := dplR::pass.filt(Q, 50, 'low')]
bcFit <- fitQmap(
  PSepAug$Qa,
  recFinal[year %in% PSepAug$year, Q],
  'RQUANT',
  wet.day = FALSE)
recFinal[, Qbc := doQmap(Q, bcFit)]

```

Figure 3

```

p1 <- ggplot(recFinal[year %in% PSepAug$year]) +
  geom_line(aes(year, Q, colour = 'Reconstruction', linetype = 'Reconstruction'), size = 0.4) +
  geom_line(aes(year, Qbc, colour = 'Bias-corrected', linetype = 'Bias-corrected'), size = 0.4) +
  geom_line(aes(year, Qa, colour = 'Observation', linetype = 'Observation'),
    PSepAug, size = 0.4) +
  scale_colour_manual(
    name = NULL,
    values = c('Observation' = 'gray30',
               'Reconstruction' = 'steelblue',
               'Bias-corrected' = 'darkorange')) +
  scale_linetype_manual(
    name = NULL,
    values = c('Observation' = 1,
               'Reconstruction' = 1,
               'Bias-corrected' = 2)) +
  scale_x_continuous(
    minor_breaks = seq(1965, 2020, 5),
    limits = c(1966, 2018),
    guide = guide_prism_offset_minor()) +
  scale_y_continuous(
    minor_breaks = seq(100, 850, 50),
    breaks = seq(100, 850, 100),
    limits = c(100, 850),
    guide = guide_prism_offset_minor()) +
  labs(x = 'Year', y = 'Precipitation [mm]', tag = 'a') +
  theme(
    plot.margin = margin(r = 10),
    legend.box.margin = margin(),
    legend.margin = margin(),
    legend.key.width = unit(2, 'cm'),
    legend.position = 'top')
p2 <- ggplot() +
  stat_density(aes(y = Q, colour = 'Reconstruction', linetype = 'Reconstruction'),
    recFinal[year %in% PSepAug$year], geom = 'line', bw = 60, size = 0.4) +
  stat_density(aes(y = Qbc, colour = 'Bias-corrected', linetype = 'Bias-corrected'),
    recFinal[year %in% PSepAug$year], geom = 'line', bw = 70, size = 0.4) +
  stat_density(aes(y = Qa, colour = 'Observation', linetype = 'Observation'),
    PSepAug, geom = 'line', bw = 70, size = 0.4) +
  scale_colour_manual(
    name = NULL,
    values = c('Observation' = 'gray30',
               'Reconstruction' = 'steelblue',
               'Bias-corrected' = 'darkorange')) +

```

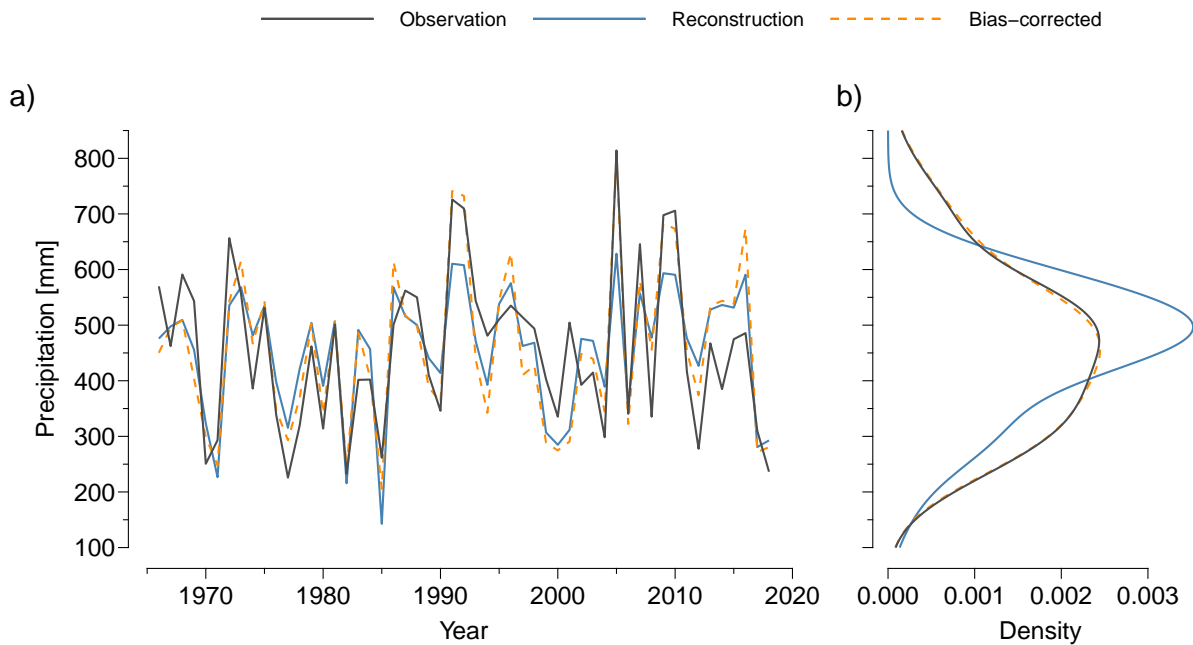
```

scale_linetype_manual(
  name = NULL,
  values = c('Observation' = 1,
             'Reconstruction' = 1,
             'Bias-corrected' = 2)) +
scale_x_continuous(guide = guide_prism_offset()) +
scale_y_continuous(
  minor_breaks = seq(100, 850, 50),
  breaks = seq(100, 850, 100),
  limits = c(100, 850),
  guide = guide_prism_offset_minor()) +
labs(y = NULL, x = 'Density', colour = NULL, tag = 'b') +
theme(
  axis.text.y = element_blank(),
  legend.box.margin = margin(),
  legend.margin = margin(),
  legend.key.width = unit(2, 'cm'),
  legend.position = 'top') +
theme(legend.position = 'top')

layout <- '
CCC
AAB
AAB
AAB
AAB
AAB
AAB
'

p1 + p2 + guide_area() +
  plot_layout(design = layout, guides = 'collect')

```



Trend and drought analyses

Calculate rolling statistics and extract drought events.

```
alignType <- 'right'
recFinal[, rolMax := frollapply(Qbc, 50, max, align = alignType)]
recFinal[, rolMin := frollapply(Qbc, 50, min, align = alignType)]
recFinal[, rolMed := frollapply(Qbc, 50, median, align = alignType)]
recFinal[, period := fcase(
  year %in% 1517:1767, 1,
  default = 2)]
densCals <- recFinal[, {
  d <- density(Qbc, cut = 0, bw = 45)
  list(x = d$x, y = d$y / max(d$y) * 1.5)
}, by = period]

medians <- recFinal[, {
  d <- density(Qbc, cut = 0, bw = 45)
  m <- median(Qbc)
  y <- approx(d$x, d$y, m)$y
  list(x = m, y = y / max(d$y) * 1.5)
}, by = period]

recFinal[, dP := Qbc - mean(Qbc),
  ][, type := classify_events(dP)
  ][, dp10 := pass.filt(dP, 10)]
droughts <- get_timing(recFinal$dP, recFinal$type)[type == 'drought']
droughts[, ':='(yearStart = recFinal[start, year],
  period = recFinal[start, period],
```



```

      yearFinal = recFinal[final, year]])
worstDroughts <- droughts[order(peak)][1:3]

```

Mann-Kendall trend test with trend-free pre-whitening.

```
recFinal[!is.na(rolMax), tfpwmk(rolMax)] |> round(6)
```

##	Z-Value	Sen's Slope	Old Sen's Slope	P-value	S
##	0.576500	0.000000	0.000000	0.564277	1844.000000
##	Var(S)	Tau			
##	10220016.000000	0.018092			

```
recFinal[!is.na(rolMin), tfpwmk(rolMin)] |> round(6)
```

##	Z-Value	Sen's Slope	Old Sen's Slope	P-value	S
##	-30.312840	-0.168350	-0.168237	0.000000	-97260.000000
##	Var(S)	Tau			
##	10294526.000000	-0.954222			

```
recFinal[!is.na(rolMed), tfpwmk(rolMed)] |> round(6)
```

##	Z-Value	Sen's Slope	Old Sen's Slope	P-value	S
##	15.055906	0.040892	0.041507	0.000000	48308.000000
##	Var(S)	Tau			
##	10294526.000000	0.473952			

Figure 4

```

p1 <- ggplot(recFinal) +
  labs(x = NULL, y = 'P [mm]') +
  geom_line(aes(year, rolMax, colour = '50-yr max'), na.rm = TRUE, size = 0.4, alpha = 0.5) +
  geom_line(aes(year, rolMin, colour = '50-yr min'), na.rm = TRUE, size = 0.4, alpha = 0.5) +
  geom_line(aes(year, rolMed, colour = '50-yr median'), na.rm = TRUE, size = 0.4, alpha = 1) +
  geom_line(aes(year, Qbc, color = 'Annual')) +
  geom_smooth(aes(year, rolMax, colour = '50-yr max'), size = 0.6,
    formula = 'y ~ x', method = 'lm', na.rm = TRUE, fill = NA) +
  geom_smooth(aes(year, rolMin, colour = '50-yr min'), size = 0.6,
    formula = 'y ~ x', method = 'lm', na.rm = TRUE, fill = NA) +
  geom_smooth(aes(year, rolMed, colour = '50-yr median'), size = 0.6,
    formula = 'y ~ x', method = 'lm', na.rm = TRUE, fill = NA) +
  scale_x_continuous(
    expand = c(0, 0),
    minor_breaks = seq(1500, 2025, 25),
    limits = c(1500, 2025),
    guide = guide_prism_offset_minor()) +
  scale_y_continuous(
    minor_breaks = seq(200, 900, 50),
    breaks = seq(200, 900, 100),
    limits = c(200, 900),
    labels = skip_label(2),

```

```

    guide = guide_prism_offset_minor()) +
  labs(x = NULL, y = 'Precipitation [mm]', colour = NULL, tag = 'a') +
  scale_color_manual(values = c(RColorBrewer::brewer.pal(3, 'Set2'), 'gray')) +
  theme(
    legend.key.width = unit(0.5, 'cm'),
    legend.position = 'top')

p2 <- ggplot(densCals) +
  geom_ribbon(aes(x, ymin = period, ymax = y + period, group = factor(period),
    fill = factor(period)),
    alpha = 0.5) +
  geom_line(aes(x, y + period, group = factor(period))) +
  geom_linerange(aes(x, ymin = period, ymax = period + y), medians, colour = 'firebrick') +
  scale_fill_manual(
    labels = c('1517-1717', '1718-2018'),
    values = wesanderson::wes_palette('Royal1', 4)[c(1, 4)]) +
  scale_x_continuous(
    guide = guide_prism_offset_minor(),
    breaks = seq(200, 900, 100),
    minor_breaks = seq(200, 900, 20)) +
  scale_y_continuous(
    expand = c(0, 0),
    breaks = c(1.5, 2.5),
    labels = c('1517-1717', '1718-2018')) +
  labs(x = 'Precipitation [mm]', y = NULL, tag = 'b') +
  theme(
    legend.position = 'none',
    axis.line.y = element_blank(),
    axis.text.y.left = element_text(angle = 90, hjust = 0.5),
    axis.ticks.y = element_blank())

p3 <- ggplot(recFinal) +
  geom_rect(
    aes(xmin = yearStart, xmax = yearFinal, ymin = -Inf, ymax = Inf),
    worstDroughts,
    fill = 'magenta4', alpha = 0.1) +
  geom_col(aes(year, dP, fill = dP), recFinal[dP > 0]) +
  scale_fill_distiller(
    palette = 'BrBG',
    limits = abs_range(recFinal$dP),
    # limits = abs_range(recFinal$dP),
    guide = guide_none(),
    direction = 1) +
  ggnewscale::new_scale_fill() +
  geom_col(aes(year, dP, fill = dP), recFinal[dP < 0]) +
  scale_fill_distiller(
    palette = 'BrBG',
    # limits = abs_range(recFinal$dP),
    limits = c(min(recFinal$dP), -min(recFinal$dP)),
    guide = guide_none(),
    direction = 1) +
  scale_color_manual(values = 'black') +
  scale_x_continuous(

```

```

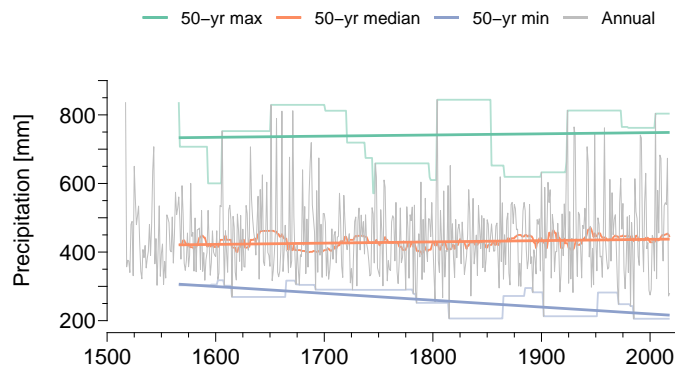
    expand = c(0, 0),
    minor_breaks = seq(1500, 2025, 25),
    limits = c(1500, 2025),
    guide = guide_prism_offset_minor()) +
scale_y_continuous(
  breaks = seq(-300, 400, 100),
  minor_breaks = seq(-300, 400, 50),
  guide = guide_prism_offset_minor()) +
labs(x = NULL, y = 'Precipitation anomaly [mm]', tag = 'c') +
theme(
  legend.position = 'top')

p4 <- ggplot(droughts) +
  geom_point(aes(dur, peak, color = as.character(period)), alpha = 0.6) +
  geom_text(
    aes(dur, peak, label = paste(yearStart, yearFinal, sep = '-')),
    worstDroughts,
    size = 2, hjust = 0.8, nudge_y = -15) +
  scale_x_continuous(
    breaks = seq(2, 20, 2),
    guide = guide_prism_offset_minor()) +
  scale_y_continuous(
    breaks = seq(-300, 0, 50),
    limits = c(-275, -25),
    guide = guide_prism_offset_minor()) +
  scale_color_manual(
    labels = c('1517-1717', '1718-2018'),
    values = wesanderson::wes_palette('Royal1', 4)[c(1, 4)] +
  labs(x = 'Drought duration [years]', y = 'Drought severity [mm]', tag = 'd') +
  theme(legend.position = 'top')

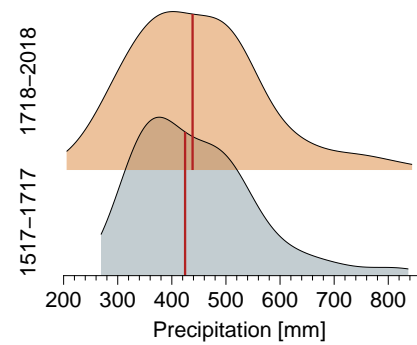
p1 + p2 + p3 + p4 +
  plot_layout(widths = c(1.5, 1))

```

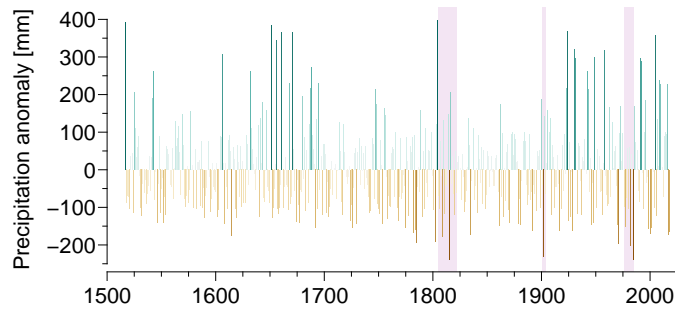
a)



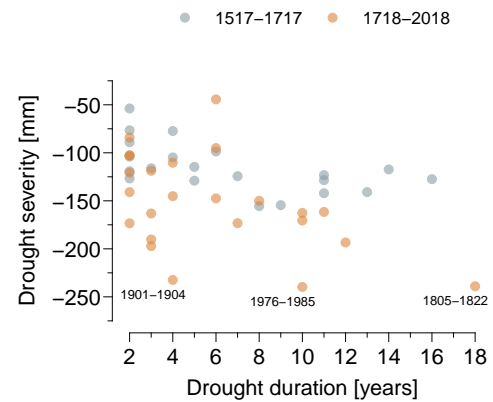
b)



c)



d)



Export the reconstruction.

```
recFinal[, period := NULL]
fwrite(
  recFinal[, .(year, P = Q, Plower = Q1, Pupper = Qu, Pbc = Qbc)],
  'results/chitral-sep-aug-precip-reconst.csv')
```